Activation of the CDC42 Effector N-WASP by the *Shigella flexneri* IcsA Protein Promotes Actin Nucleation by Arp2/3 Complex and Bacterial Actin-based Motility

Coumaran Egile,[‡] Thomas P. Loisel,[§] Valérie Laurent,[§] Rong Li,[*] Dominique Pantaloni,[§] Philippe J. Sansonetti,[‡] and Marie-France Carlier[§]

*Department of Cell Biology, Harvard Medical School, Boston, Massachusetts 02115; [‡]Unité de Pathogénie Microbienne Moléculaire, INSERM U 389, Institut Pasteur, 75724 Paris Cedex 15; and [§]Dynamique du Cytosquelette, Laboratoire d'Enzymologie et Biochimie Structurale, Centre National de la Recherche Scientifique, Gif-sur-Yvette, 91198 France

Abstract. To propel itself in infected cells, the pathogen *Shigella flexneri* subverts the Cdc42-controlled machinery responsible for actin assembly during filopodia formation. Using a combination of bacterial motility assays in platelet extracts with *Escherichia coli* expressing the *Shigella* IcsA protein and in vitro analysis of reconstituted systems from purified proteins, we show here that the bacterial protein IcsA binds N-WASP and activates it in a Cdc42-like fashion. Dramatic stimulation of actin assembly is linked to the formation of a ternary IcsA–N-WASP–Arp2/3 complex, which nucleates actin polymerization. The Arp2/3 complex is essential in initiation of actin assembly and *Shigella* movement, as previously observed for *Listeria monocytogenes*. Activation of N-WASP by IcsA unmasks two domains acting together in insertional actin polymerization. The isolated COOH-terminal domain of N-WASP containing a verprolin-homology region, a cofilin-homology sequence, and an acidic terminal segment (VCA) interacts with G-actin in a unique profilin-like functional fashion. Hence, when N-WASP is activated, its COOH-terminal domain feeds barbed end growth of filaments and lowers the critical concentration at the bacterial surface. On the other hand, the NH_2-terminal domain of N-WASP interacts with F-actin, mediating the attachment of the actin tail to the bacterium surface. VASP is not involved in *Shigella* movement, and the function of profilin does not require its binding to proline-rich regions.

Key words: *Shigella flexneri* • IcsA • N-WASP • Arp2/3 complex • actin

THE motile response of living cells to extracellular stimuli is mediated by a highly integrated signaling cascade that transduces external signals to the actin cytoskeleton to elicit spatially controlled actin polymerization. Many of the components playing a role in this cascade have been identified. Among them, Rho, Rac, and Cdc42, small GTPases of the Rho family, act as molecular regulators of actin assembly and control the formation of focal adhesions, lamellipodia, and filopodia, respectively (Kozma et al., 1995; Nobes and Hall, 1995). On the other hand, the molecular mechanisms connecting Rac and Cdc42 to actin filament assembly during cell locomotion are still unknown.

Intracellular actin-based propulsion of pathogens provides an invaluable tool for the mechanistic analysis of the small GTPase effectors involved in the regulation of actin assembly (Beckerle, 1998). *Shigella flexneri*, *Listeria monocytogenes*, or the vaccinia virus (Higley and Way, 1997) induce polarized constitutive actin assembly at their surface into a reticulated meshwork (Bernardini et al., 1989; Prevost et al., 1992; Goldberg et al., 1993; Nhieu and Sansonetti, 1999 for a recent review), and use the resulting propulsive force to move at rates of 1–50 μm/min and spread from cell to cell by membrane invagination and lysis. A single bacterial surface protein, ActA on *Listeria* (Domann et al., 1992; Kocks et al., 1992), or IcsA (VirG) on *Shigella* (Bernardini et al., 1989; Lett et al., 1989), is necessary and sufficient (Goldberg and Theriot, 1995; Kocks et al., 1995) to induce actin-based motility of the bacterium. The *Listeria* system has been extensively studied. The multidomain ActA protein recruits two essential factors in motility. The NH_2-terminal domain of ActA interacts with the Arp2/3 complex (Welch et al., 1997) and activates its actin nucleating activity (Welch et al., 1998). The central proline-rich domain of ActA interacts with the

C. Egile and T.P. Loisel contributed equally to this work.

Address correspondence to M.-F. Carlier, Dynamique du Cytosquelette, LEBS, CNRS, Gif-sur-Yvette, 91198 France. Tel.: (33) 1 69 82 31 65. Fax: (33) 1 69 82 34 65. E-mail: carlier@lebs.cnrs-gif.fr

focal adhesion protein VASP (Smith et al., 1996; Niebuhr et al., 1997), which links the actin tail to the bacterium surface, allowing directed insertional polymerization (Laurent et al., 1999).

Although the IcsA protein has no sequence similarity to ActA, the physical features of *Shigella* actin-based movement are identical to *Listeria*, suggesting that at least some of the key players involved in movement are the same in the two systems. Two proteins have been reported to interact with IcsA, vinculin (Suzuki et al., 1996) and N-WASP (Suzuki et al., 1998). Vinculin was postulated to associate with VASP via its ActA-like proline-rich segment, suggesting that VASP would play in *Shigella* movement the same role as in *Listeria* (Laine et al., 1997). However, *Shigella* moves well in cells that do not express vinculin (Goldberg, 1997). N-WASP is a member of the WASP family of proteins, which thus far includes Las17/Bee1 in *Saccharomyces cerevisiae* (Lechler and Li, 1997; Li, 1997); Scar1/WAVE in *Dictyostelium discoideum*, *Caenorhabditis elegans*, *Drosophila melanogaster*, mouse, and humans (Bear et al., 1998; Miki et al., 1998a); and WASP (Derry et al., 1994) and its close homologue N-WASP (Miki et al., 1996) in humans. Mutations in the WASP protein result in the Wiskott-Aldrich syndrome (Ramesh et al., 1999). Among WASP-related proteins, only WASP and N-WASP contain a consensus CRIB motif for Cdc42 binding. N-WASP enhances Cdc42-induced formation of filopodia (Miki et al., 1998b). It has been proposed that N-WASP is activated by the N-WASP–Cdc42 interaction. In vitro, Cdc42 drives actin polymerization in acellular extracts (Ma et al., 1998a; Zigmond et al., 1998). WASP and N-WASP therefore are thought to link Cdc42 to actin polymerization (Bi and Zigmond, 1999, for a recent review). Proteins of the WASP family also contain a proline-rich region thought to bind SH3 domains, as well as profilin (Suetsugu et al., 1998), and a COOH-terminal domain containing a verprolin-homology region, a cofilin-homology sequence, and an acidic terminal segment (VCA)[1]. The actin filament severing and depolymerizing activities of the VCA region are thought to be involved in microspike formation (Miki et al., 1998b) and in actin-based motility of *Shigella* (Suzuki et al., 1998).

The recent discovery that the acidic extreme COOH-terminal region of Scar1 interacts with p21-Arc, a component of the Arp2/3 complex (Machesky and Insall, 1998), and enhances its actin nucleating activity (Machesky et al., 1999) was a landmark in the field. The Arp2/3 complex then was reported to mediate actin polymerization induced by Cdc42 (Ma et al., 1998b). Recently, activation of Arp2/3 by N-WASP was found enhanced by Cdc42 (Rohatgi et al., 1999). In yeast, the Arp2/3 complex is activated by the COOH-terminal domain of Bee1p (Winter et al., 1999). However, the molecular mechanism for site-directed actin assembly and production of force and movement remains unknown.

The goal of our work was to understand how the different components of the actin assembly machinery are sequentially switched on to elicit actin nucleation and insertional polymerization to produce *Shigella* movement. To address this issue, we have used a combination of bacterial motility assays using IcsA-expressing *Escherichia coli* in platelet and brain extracts, immunodepletion and add-back methods, and in vitro steady state and kinetic measurements of actin polymerization in the presence of individual and combined components of the machinery, using purified IcsA, N-WASP, VCA, Arp2/3 complex, Cdc42, VASP, and wild-type and mutated profilins. We've come up with a working model for *Shigella* movement that provides a general insight into the mechanism of actin-based cellular extensions.

Materials and Methods

Bacterial Strains

E. coli BUG 968 strain and BUG 896 strain expressing the membrane form of IcsA (BUG 968 harboring pHS3199, a pUC8 plasmid containing *IcsA* gene; Kocks et al. 1995) were grown at 37°C in 2YT in the presence of 100 μg/ml ampicillin until midexponential phase was reached. *Listeria* strain Lut12 (pActA3) overexpressing ActA (Kocks et al., 1992) was grown at 37°C in brain/heart infusion medium in the presence of 7 μg/ml chloramphenicol and 5 μg/ml erythromycin until midexponential phase was reached. Bacteria were kept frozen in 30% glycerol at −80°C.

Antibodies

Polyclonal rabbit antibodies were raised against human N-WASP protein residues ^{473}-EVMQKRSKAIHSSDED-^{488} (C412 antibodies) and against recombinant human N-WASP protein obtained from baculovirus (NW011 antibodies). Anti-Arp3 polyclonal antibodies (AR3) were raised in rabbits against Arp3 residues YEEIGPSIVRHNPVFGVMS. Affinity-purified C421, NW011, and AR3 antibodies were used for Western blot and immunofluorescence, respectively, at 10 μg/ml concentration. Antibovine profilin polyclonal antibodies were raised in rabbits and used in Western blots at a 1:5,000 dilution.

Platelet and Brain Extracts

Human platelet extracts were prepared from outdated unstimulated preparations as previously described (Laurent and Carlier, 1997). Bovine brain extracts were prepared as follows. Brain was homogenized in 1 vol of 0.1 M MES, pH 6.8, 1 mM EGTA, 0.5 mM $MgCl_2$, 0.1 mM EDTA, 1 mM DTT, and clarified by centrifugation at 10,000 *g* for 30 min at 4°C. Tubulin and neurofilaments were removed by centrifugation for 1 h at 150,000 *g* after one cycle of microtubule assembly at 37°C for 30 min in the presence 0.5 mM GTP, 4 M glycerol, and 0.25 mM $MgCl_2$. The supernatant (S_2) was stored at −80°C.

Recombinant Proteins Expression and Purification

Histidine-tagged human N-WASP was expressed in High Five insect cells. Human cDNA was cloned in pFast Bac Htb (Life Technologies, Inc.) and recombinant baculovirus constructed using standard protocol of transfection–recombination in insect cell lines. High Five insect cells were infected at a multiplicity of infection of 2. Cell culture was performed in suspension, in High Five serum-free medium, under vigorous shaking at 27°C for 40 h. Protein purification was performed by DEAE cellulose at pH 7.8 and cobalt affinity chromatography, as described by Laurent et al. (1999). Recombinant histidine-tagged human VASP was expressed and purified as described previously (Laurent et al., 1999).

The NH_2-terminal (Nt) and COOH-terminal domains (VCA) of human N-WASP were expressed and purified as GST fusion proteins in *E. coli*. Human cDNA regions encoding N-WASP Nt (residues 1-276) and VCA (residues 392-505) were amplified by PCR from human brain cDNA using oligonucleotides phNW1 (5′-ccggaattcATGAGCTCCGTCCAGCAGCAG-3′), phNW276 (5′-ccgctcgagTCACTTGCCTCCGCAGTTCATTTTTAAC-3′), and oligonucleotides phNW392 (5′-ccggaattcCCTTCTGATGGGGACCATCAG-3′), phNW505 (5′-ccgctcgagTCAGTCTTCCCACTCATCATC-3′), respectively. N-WASP Nt and VCA PCR

1. *Abbreviations used in this paper:* AR3, anti-Arp3 polyclonal antibodies; K_d, dissociation constant; Nt, NH_2-terminal domain; VCA, COOH-terminal domain containing a verprolin-homology region, a cofilin-homology sequence, and an acidic terminal segment.

fragments were cloned in EcoRI and XhoI sites in pGEX4T-1 plasmid, respectively, to generate pCENHN and pCECHN plasmids. GST-Nt and GST-VCA protein expressions were obtained using BL21 *E. coli* strain according to standard induction and purification procedures. GST-Nt and GST-VCA glutathione Sepharose beads were kept at 4°C until use. GST-Nt protein was eluted from beads and VCA protein was obtained by thrombin cleavage. Both proteins were dialyzed against 10 mM Tris-Cl^-, pH 7.5, 1 mM DTT, 50 mM KCl, and 0.01% NaN_3, frozen on liquid nitrogen and stored at −80°C. The concentration of VCA was determined spectrophotometrically using an extinction coefficient $\epsilon_{0.1\%}$ of 0.467 cm^{-1} at 278 nm calculated from the amino acid sequence, and a mol wt of 12,900 D. Due to the acidic character of VCA, the Bradford protein assay gave underestimated values of the concentration.

Human Cdc42 was also expressed as a GST fusion protein in *E. coli.* Human cDNA was cloned in pGEX2T expression plasmid and was a kind gift from Dr. Alan Hall (Medical Research Council, University College, London, UK). Protein was expressed in *E. coli* JM109, purified on glutathione Sepharose as described, and kept on beads at 4°C in 10 mM Tris-Cl^-, pH 7.6, 150 mM NaCl, 2 mM $MgCl_2$, 0.1 mM DTT, and 0.1 mM GTP. When required, GST-Cdc42 was loaded with GDP or GTPγS on beads by a 1-h incubation at room temperature on a wheel in 50 mM Tris-Cl^-, pH 7.6, 150 mM NaCl, 2 mM $MgCl_2$, 1 mM DTT, 10 mM EDTA, and 0.1 mM GDP or GTPγS. The exchange reaction was stopped by addition of 10 mM $MgCl_2$.

$IcsA_{53\text{-}508}$ protein was purified as a GST fusion protein as described in Suzuki et al. (1996).

Purification of Arp2/3 Complex from Bovine Brain

Bovine Arp2/3 complex was purified from bovine brain extracts by a novel two step method as follows. 100 ml of S_2 was dialyzed against 50 mM MES, pH 6.8, containing 1 mM DTT, 1 mM EDTA, and 1 mM $MgCl_2$ (buffer A), and loaded on an SP-Trisacryl column (2.5 × 12 cm) equilibrated in buffer A. After a wash step with 30 mM KCl, the Arp2/3 complex was eluted with 80 mM KCl in buffer A. This fraction was equilibrated in 20 mM Tris-Cl^-, pH 7.5, containing 25 mM KCl, 1 mM DTT, 1 mM $MgCl_2$, 0.5 mM EDTA, and 0.1 mM ATP-Tris, pH 7.5 (buffer B), and loaded on a GST-VCA glutathione Sepharose column (0.5 × 1 cm) in buffer B. Most of the proteins were washed off the column by buffer B, the remaining non-Arp2/3 proteins were eluted by 0.2 M KCl in buffer B, pending a small loss of Arp2/3 activity, and the pure Arp2/3 complex was eluted with 0.2 M $MgCl_2$ in buffer B (see Fig. 2 b for the purity of the Arp2/3 complex). After dialysis against buffer B, the protein was concentrated using a Centriprep 30 cartridge (Amicon). The Arp2/3 complex was supplemented with 0.2 M sucrose and stored at −80°C. The activity of Arp2/3 along the purification steps was monitored spectrofluorimetrically, using the ability of Arp2/3 to activate the branched polymerization of actin filaments in the presence of VCA. The assay (80 μl) contained 2.5 μM Mg-G-actin (10% pyrenyl-labeled), 0.5 μM VCA, and 10 μl of the tested fraction in 5 mM Tris-Cl^-, pH 7.8 buffer, 1 mM DTT, 0.2 mM ATP, 0.1 M KCl, and 1 mM $MgCl_2$. The time course of increase in pyrenyl-actin fluorescence was followed. The activity of Arp2/3 was detected by the steep sigmoidal increase in fluorescence, indicative of branched polymerization. The activity of Arp2/3 was easily observed, even in the S_2 fraction. Alternatively, the activity of Arp2/3 was detected by the video-microscopy bacterial motility assay, using the property of Arp2/3 to initiate the formation of actin clouds at the surface of *Listeria* incubated in 4 μM rhodamine-labeled actin. The results of the two tests were in good agreement with each other, but the spectrofluorometric assay was more convenient and easily amenable to a quantitative estimate of the amount of Arp2/3 in the tested fractions by comparison with a calibration series of time courses performed with known concentrations of pure Arp2/3. The concentration of Arp2/3 complex was determined spectrophotometrically using an extinction coefficient of 224,480 $M^{-1} \cdot cm^{-1}$ at 278 nm, derived from the amino acid sequence of the seven polypeptides composing the 223,949-D complex. A good agreement was obtained between the spectrophotometric measurement and the bicinchoninic acid assay, with BSA as a standard. Typically, 1.2 nmol (0.26 mg) of pure Arp2/3 complex was obtained from 100 ml brain S_2 supernatant.

Depletion of Arp2/3 Complex, VASP, and Profilin from Platelet Extracts

Arp2/3 complex was depleted from platelet extracts using a variation of the coprecipitation method described by Machesky and Insall (1998). Various amounts of glutathione Sepharose-coupled GST-VCA beads (20, 40, and 80 μg) were incubated with 25 μl of platelet extracts for 30 min at 4°C on a rotating wheel. Beads were pelleted at 5,000 *g* for 15 s. Depletion of the Arp2/3 complex was monitored by Western blotting of aliquots of protein extracts and beads. Add-back was done using the Arp2/3 complex purified from bovine brain.

VASP immunodepletion was carried out as described previously (Laurent et al., 1999). Add-back was done using the recombinant VASP purified from insect cells.

Profilin depletion was carried out by two consecutive poly-L-proline chromatography steps, as described by Laurent et al. (1999). Profilin depletion was monitored by Western blotting. Add-back was done using the purified wild-type profilin or the H133S mutant profilin, described as unable to bind poly-L-proline (Bjorkegren-Sjogren et al., 1997).

Actin and Regulatory Proteins

Actin was purified from rabbit muscle and isolated as Ca-ATP-G-actin by gel filtration on Sephadex G-200 in G buffer (5 mM Tris-Cl^-, pH 7.8, containing 0.1 mM $CaCl_2$, 0.2 mM ATP, and 1 mM DTT). Actin was pyrenyl- or rhodamine-labeled, and converted into Mg-G-actin before polymerization, as described by Carlier et al. (1997). Mg-actin was polymerized by addition of 1 mM $MgCl_2$ and 0.1 M KCl (physiological ionic conditions). When actin was polymerized in the presence of gelsolin, no EGTA was added to the solution, and Ca-ATP-G-actin supplemented with the desired amount of gelsolin was polymerized by addition of 2 mM $MgCl_2$ and 0.1 M KCl.

Thymosin β4 was purified from bovine spleen as described by Pantaloni and Carlier (1993).

Gelsolin purified from human plasma was a kind gift from Dr. Yukio Doi (University of Kyoto, Kyoto, Japan).

Spectrin-actin seeds were isolated from human erythrocytes as described by Casella et al. (1986).

Actin Polymerization Assays

Critical concentration plots were performed by serial dilution of pyrenyl-labeled F-actin solutions in F buffer (5 mM Tris-Cl^-, pH 7.8, containing 1 mM DTT, 0.2 mM ATP, 0.1 mM $CaCl_2$, 1 mM $MgCl_2$, and 0.1 M KCl) and incubated overnight at room temperature. Polymerization assays were performed using the change in pyrenyl-actin fluorescence. Measurements were carried out in a Spex Fluorolog 2 instrument thermostated at 20°C, with excitation and emission wavelengths of 366 and 407 nm, respectively, and appropriate filters placed on the excitation and emisssion beams to eliminate stray light and bleaching, which interfere in polymerization in the presence of Arp2/3 (Pantaloni, D., manuscript in preparation).

The G-actin sequestering activity was measured by the shift in critical concentration plots with gelsolin-capped filament barbed ends. The equilibrium dissociation constant, K_d, for the actin-sequestering protein complex was derived from the measurements of the concentration, $[A_0]$, of unassembled actin at steady state (abscissa intercept of the critical concentration plots) and of the critical concentration, $[A_C]$, determined in the absence of sequestering agent. The following equation was used: $K_d = [A_C] \cdot ([S_0] - [A_0] + [A_C]) / ([A_0] - [A_C])$, in which $[S_0]$ represents the total concentration of sequestering protein.

Rates of filament growth from barbed and pointed ends were measured using spectrin–actin seeds or gelsolin-capped filaments, added at time zero to a solution of 1 μM MgATP–G-actin (10% pyrenyl-labeled) in polymerization buffer. The gelsolin-capped filament solution contained 5 μM F-actin polymerized in the presence of 16.7 nM gelsolin for 2 h, and diluted 20-fold into the G-actin solution.

Motility Assays

Frozen bacteria were thawed and spun down at 4,000 *g* for 5 min at 22°C, resuspended at 6×10^9 bacteria/ml in XB buffer (10 mM Hepes, pH 7.7, 0.1 M KCl, 1 mM $MgCl_2$, 0.1 mM $CaCl_2$, and 50 mM sucrose). Motility assays were performed by mixing 4 μl of thawed extracts supplemented with 12 μl of a mixture containing 5 μM F-actin, 0.38% methyl cellulose, 6 mM DTT, 2 mM ATP/$MgCl_2$, 1.5×10^{-3}% DABCO, 1 μM rhodamine-actin, and 2×10^8 bacteria/ml. An aliquot of 2.5 μl was squashed between a 22 × 22 mm coverslip and a slide, sealed with VALAP, and incubated for 5 min at room temperature before motility measurements. Fluorescence microscopy observations and data acquisition were carried out as previously described (Laurent et al., 1999). N-WASP-coated *E. coli* (IcsA) were prepared as follows: 20 μl of a suspension of 6×10^9 bacteria/ml were incubated with 5 μl of 1 μM N-WASP for 5 min at room temperature.

Bacteria were pelleted, washed, and resuspended in 20 μl of XB buffer and kept on ice. The N-WASP–IcsA complex remains stable for several hours on ice.

Immunofluorescence Analysis of Shigella-infected HeLa Cells

HeLa cells were infected as follows: overnight culture of *Shigella* M90T strain was diluted in tryptic soy broth, grown to midexponential phase, centrifuged at 5,000 *g* for 5 min, washed, and resuspended at 10^8 bacteria/ml (M90T) in MEM, 50 mM Hepes, pH 7.5. HeLa cells, seeded on glass coverslips, were washed three times with MEM, overlaid with the bacterial suspension, and centrifuged for 10 min at 800 *g*. Bacterial entry was allowed by 30 min incubation at 37°C. Infected cells were washed with MEM five times and incubated with MEM, 50 mM Hepes, pH 7.5, with 50 μg/ml of gentamicin for a further 1 h at 37°C, to allow intracellular spread.

For immunofluorescence staining, infected cells were permeabilized with 0.2% Triton X-100 in 0.1 M MES, pH 7.4, 1 mM $MgCl_2$, 1 mM EGTA, 4% PEG 6000, and then fixed for 30 min in 3.7% paraformaldehyde in PBS. After quenching with NH_4Cl 50 mM in PBS for 10 min and saturation for 30 min in PBS-BSA 2%, infected cells were incubated with specific mono- or polyclonal antibodies. Affinity-purified antihuman N-WASP polyclonal NW011 antibodies and polyclonal Arp3 antibodies were used at 10 μg/ml concentration. Texas red-conjugated secondary antibodies (Nycomed Amersham Inc.) were used. F-actin was visualized by FITC-phalloidin (0.1 mg/ml; Sigma Chemical Co.). Preparations were examined with a confocal laser scanning microscope (Zeiss Axiophot).

In Vitro Protein Binding Assays

Glutathione Sepharose coupled to GST–IcsA or to GST was equilibrated in buffer P (20 mM Tris-Cl^-, pH 7.5, 100 mM KCl, 1 mM $MgCl_2$, and 0.1% BSA). 100 pmol of protein-bound beads and 80 pmol of purified N-WASP or VCA were mixed in 100 μl (total vol) and incubated for 1 h at 4°C on a rotating wheel. Supernatants were collected. Beads were rinsed twice with buffer P. Free and bound N-WASP and VCA were detected by Western blotting after resolving the proteins by SDS-PAGE.

Results

Association of N-WASP to IcsA Is Required for Actin-based Motility of E. coli (IcsA) in Platelet Extracts

Actin-based motility of *E. coli* (IcsA) has been observed in *Xenopus* egg extracts (Goldberg and Theriot, 1995; Kocks et al., 1995, Suzuki et al., 1998). Motility was observed as well in HeLa cell extracts and murine or bovine brain extracts, but not at all in human platelet extracts, which, in contrast, supports actin-based motility of *Listeria*. This puzzling observation suggested that an essential factor for *Shigella* motility is missing in platelets. The requirement of N-WASP for *Shigella* motility in *Xenopus* egg extracts has recently been demonstrated (Suzuki et al., 1998). Immunoblotting using polyclonal NW 011 antibodies that recognize both WASP and N-WASP (Fig. 1 a), showed that N-WASP was present in brain extracts, but absent in platelets, which, in contrast, contain the lower molecular weight WASP homologous protein mainly expressed in hematopoietic cells (Fig. 1 a), whose mutations result in the Wiskott-Aldrich syndrome (Ramesh et al., 1999). The endogenous WASP protein, homologue of N-WASP in platelets, apparently cannot bind IcsA. To check whether the absence of N-WASP was responsible for the lack of *E. coli* (IcsA) motility in platelet extracts, recombinant human N-WASP was expressed using the baculovirus system and purified (Fig. 1 b). The interaction of recombinant N-WASP with IcsA was verified by successful binding of N-WASP on glutathione Sepharose beads to which the GST–IcsA fusion protein was attached (Fig. 1 c). The isolated VCA of N-WASP, in contrast, did not bind to IcsA (Fig. 1 c). Actin-based motility of *E. coli* (IcsA) was restored by addition of N-WASP to platelet extracts. Specifically, upon addition of 10 nM N-WASP, actin clouds were observed. Comets were observed upon addition of 50 nM N-WASP, optimum movement was seen at 100 nM N-WASP, and inhibition occurred at 1 μM N-WASP. Neither bacterial motility nor actin polymerization were observed under the same conditions with control BUG 968 *E. coli* bacteria that did not express IcsA (see Materials and Methods). Consistent with the apparent high affinity of N-WASP for IcsA, when *E. coli* (IcsA) bacteria were incubated with N-WASP at concentrations as low as 0.1 μM, washed, and added to platelet extracts, bacterial actin-based motility was readily observed (Fig. 1 d). Bacteria induced actin polymerization and moved at rates similar to *Listeria* (4 μm/min, SD = 1, $n = 20$). In contrast, when control BUG 968 *E. coli* bacteria that did not express IcsA were preincubated with N-WASP, washed, and added to platelet extracts, they failed to induce actin assembly and to move. Consistent with these results, beads coated with GST–$IcsA_{53\text{-}508}$ induced actin assembly at their surface in platelet extracts only when they were first preincubated with N-WASP (Fig. 1 e). Control GST beads, preincubated in the same N-WASP solution, and washed, failed to induce actin assembly in platelet extracts. Neither actin assembly nor movement was observed when bacteria or GST–IcsA beads were preincubated with VCA instead of N-WASP. Accordingly, bacterial movement and actin assembly were not inhibited by the presence of a 20-fold molar excess of VCA over N-WASP in the preincubation step. Hence, VCA does not displace IcsA-bound N-WASP.

These results demonstrate that interaction of IcsA with N-WASP is crucial for IcsA-mediated actin polymerization and bacterial motility, and that VCA does not interact with IcsA.

Association of Arp2/3 Complex with N-WASP Bound to IcsA at the Surface of E. coli (IcsA) Is Necessary and Sufficient for Initiation of Actin Assembly

The N-WASP protein was proposed to initiate actin assembly at the surface of bacteria by interacting with actin via its two verprolin homology regions and/or its cofilin homology sequence (Miki et al., 1998b; Suzuki et al., 1998). However, when either the *E. coli* (IcsA) bacteria or the GST–IcsA beads precoated with N-WASP were incubated in a solution of rhodamine-labeled F-actin, no initiation of actin assembly was observed at their surface (data not shown), indicating that, in itself, the actin-binding property of N-WASP is not sufficient for inducing the actin assembly seen in platelet extracts.

Recently, the association of the Arp2/3 complex with Scar1, a member of the WASP family, was demonstrated to enhance the actin nucleation activity of Arp2/3 complex in vitro (Machesky and Insall, 1998; Machesky et al., 1999). To investigate the role of Arp2/3 complex in *Shigella* motility, platelet extracts were at least 80% depleted in Arp2/3 complex by GST-VCA beads (Fig. 2 a). Actin polymerization and motility of *E. coli* (IcsA) coated with

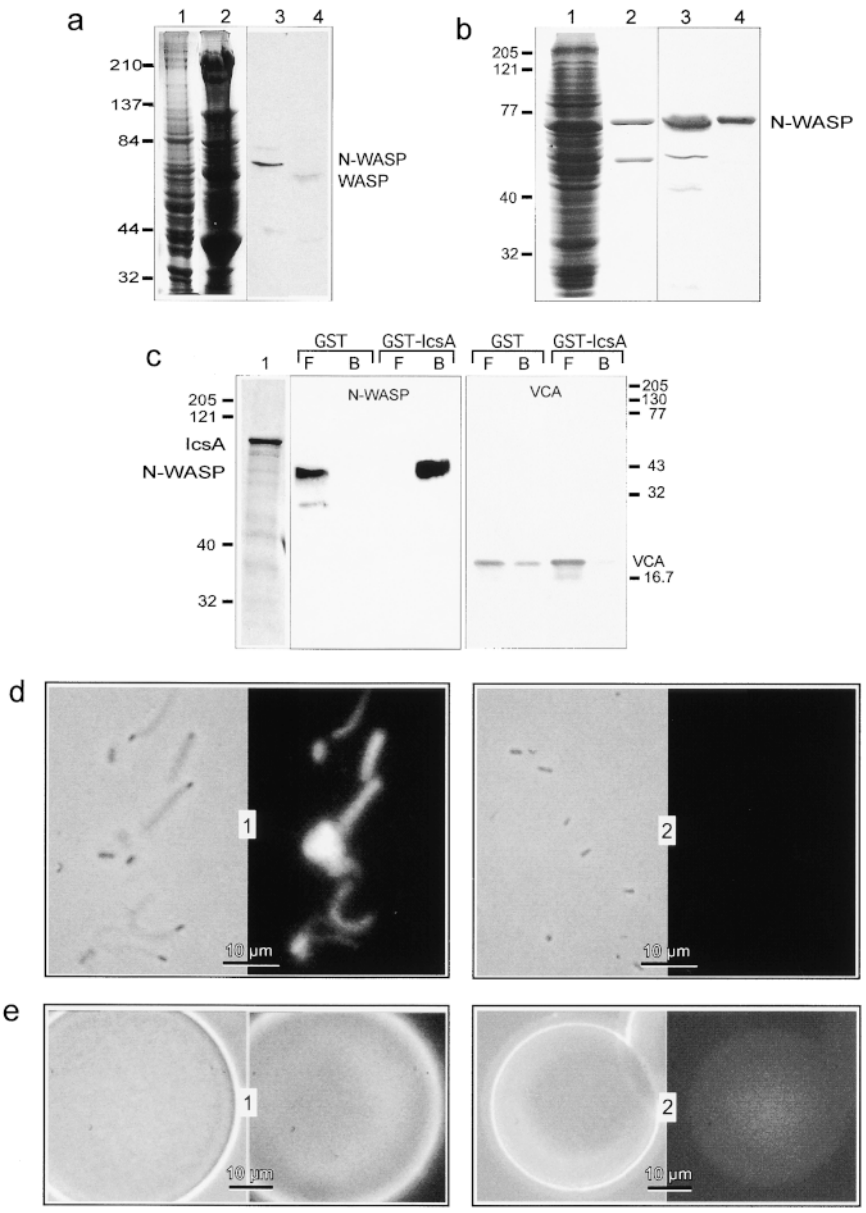

Figure 1. N-WASP is required for actin-based motility of *E. coli* (IcsA). a, N-WASP is not detected in platelet extracts. N-WASP expression was analyzed by SDS-PAGE in brain extracts (lanes 1 and 3) and in platelet extracts (lanes 2 and 4). Lanes 1 and 2, Coomassie blue staining; lanes 3 and 4, immunoblotting with anti-N-WASP. Note the presence of WASP, but no N-WASP, in platelets (lane 4). b, Purified recombinant histidine-tagged human N-WASP protein. SDS-PAGE patterns of insect cell extracts (lanes 1 and 3) and purified recombinant human N-WASP (lanes 2 and 4). Lanes 1 and 2, Coomassie blue staining; lanes 3 and 4, immunoblotting with anti-N-WASP. c, Full-length N-WASP, but not the isolated VCA, binds to IcsA. GST–$IcsA_{53\text{-}508}$ or GST beads were incubated with N-WASP or VCA in a pull-down assay. Free protein (F) and protein bound to the beads (B) were detected by immunoblotting with C412 anti N-WASP polyclonal antibodies. Lane 1, SDS-PAGE (Coomassie blue staining) of GST–IcsA. d, Binding of N-WASP to *E. coli* (IcsA) induces bacterial motility in platelet extracts. 1, Actin tails formed by N-WASP–coated *E. coli* (IcsA) incubated in platelets extracts; 2, absence of actin tails upon incubation of *E. coli* (IcsA) in platelet extracts; left panels, phase-contrast; right panels: rhodamine-actin fluorescence. Bars, 10 μm. e, Actin polymerization is induced at the surface of Sepharose-coupled GST–$IcsA_{53\text{-}508}$ beads coated with N-WASP. Actin polymerization occurs at the surface of Sepharose-coupled GST–$IcsA_{53\text{-}508}$ beads when recombinant N-WASP is added to platelet extracts (1). No polymerization is detected in the absence of N-WASP (2). Left panels: phase-contrast; right panels: rhodamine-actin fluorescence. Bars, 10 μm.

N-WASP and of *Listeria* were completely abolished in those Arp2/3-depleted extracts. Add-back of 0.15 μM pure Arp2/3 from bovine brain to the depleted platelet extracts restored bacterial movement at a rate of 1 ± 0.2 μm/min, i.e., 30% of the speed observed in the mock-depleted extracts.

The N-WASP–coated *E. coli* (IcsA) bacteria, N-WASP–bound GST–IcsA beads, or *Listeria* bacteria were then incubated in a solution of rhodamine-labeled F-actin containing pure Arp2/3 from bovine brain (Fig. 2 b). Formation of actin clouds around the bacteria and the beads was immediately observed (Fig. 2 c). These results demonstrate that IcsA-bound N-WASP interacts with Arp2/3 complex, and that the IcsA–N-WASP–Arp2/3 complex is able to initiate local actin assembly in a solution of pure actin. Previously, we have shown, using phalloidin, that G-actin, not F-actin, was recruited by Arp2/3 at the *Listeria* surface (Marchand et al., 1995). Even though actin was polymerized in the assay, it is the G-actin that coexists at steady state with the filaments that are shuttled onto barbed ends created by Arp2/3.

To get more insight into the respective roles of N-WASP and Arp2/3 in *Shigella* movement, immunolocalization of the two proteins in infected cells was carried out. N-WASP colocalized with IcsA at the surface of *Shigella*, whereas the Arp2/3 complex was found in the entire actin tail (Fig. 3). In conclusion, Arp2/3 interacts with N-WASP to initiate actin assembly at the surface of Shig*ella*, but the interaction of Arp2/3 with N-WASP is not permanent, and the Arp2/3 complex remains incorporated into the assembled filaments. In contrast, the interaction of N-WASP with IcsA is probably very strong and in slow equilibrium.

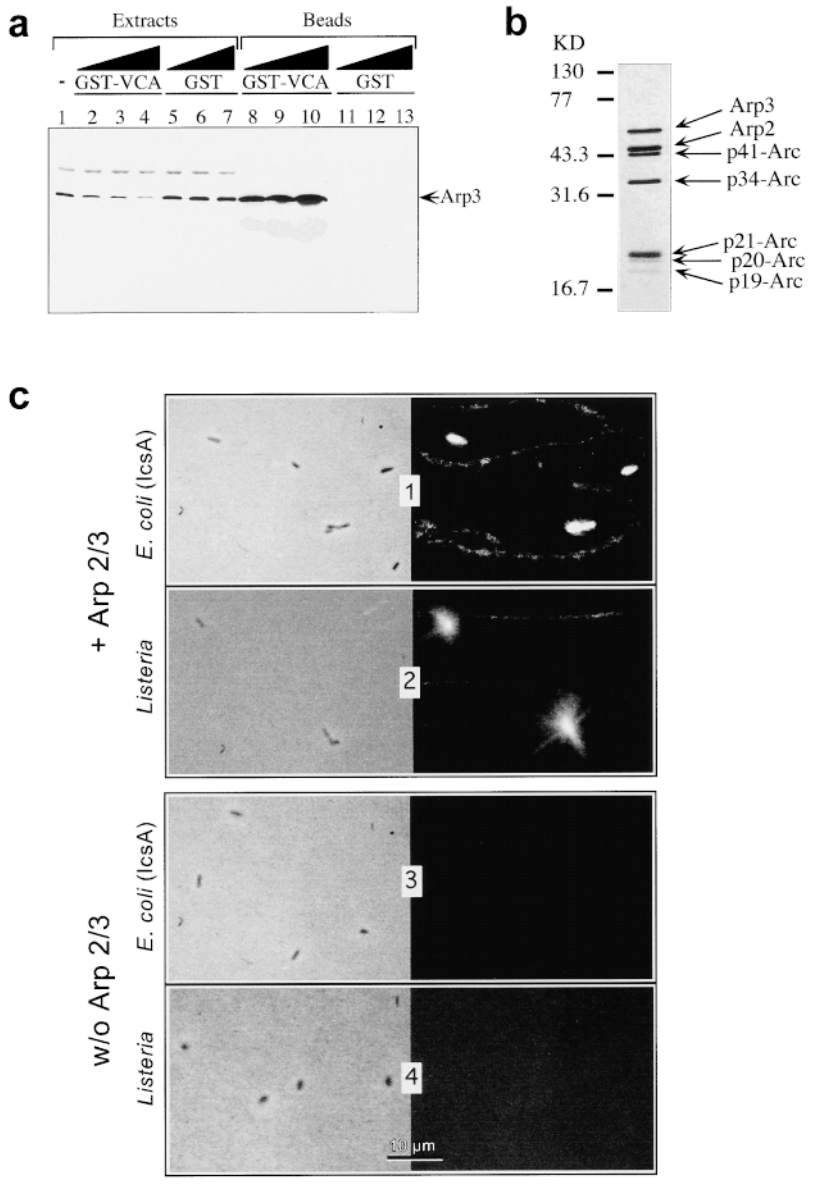

Figure 2. Arp2/3 complex is essential for actin nucleation at the surface of *E. coli* (IcsA) and *Listeria*. a, Arp2/3 complex depletion in platelet extracts. Increasing amounts (20, 40, and 80 μg) of glutathione Sepharose-coupled GST or GST-VCA beads were incubated with 25 μl of platelet extracts. Arp2/3 depletion is monitored by immunoblotting using anti-Arp3 polyclonal antibody. 1, Arp3 in untreated platelet extracts; 2–4, Arp2/3-depleted extracts; 5–7, mock-depleted extracts; 8–10, Arp3 associated with GST-VCA beads; and 11–13, Arp3 associated with GST beads. b, VCA affinity-purified Arp2/3 complex from bovine brain. The composition of the Arp2/3 complex is shown. The seven polypeptides are detected by Coomassie blue staining after SDS-PAGE. c, In vitro reconstitution of actin filaments assembly on *E. coli* (IcsA) and *Listeria* surface. N-WASP–coated *E. coli* (IcsA) or *Listeria* were incubated in a solution of pure rhodamine-labeled F-actin (10 μM) with or without 0.15 μM pure Arp2/3 complex as indicated. Left panels, phase-contrast; right panels, fluorescence. Bar, 5 μm.

N-WASP Enhances the Actin Nucleation Activity of Arp2/3 in a Cdc42-activated Fashion

To understand how the interaction between IcsA-bound N-WASP with Arp2/3 complex leads to the initiation of actin filament assembly at the surface of *Shigella*, the biochemical properties of the individual proteins of this complex machinery were examined in in vitro experiments. The Arp2/3 complex purified from bovine brain was able to induce the branched polymerization of actin filaments (Ressad et al., 1999), like the *Acanthamoeba* complex (Mullins et al., 1998). The activity of the Arp2/3 complex appeared enhanced by either the VCA domain of N-WASP (Fig. 4 a) or by the entire N-WASP protein (Fig. 4 b) in the same concentration-dependent manner. At 2.5 μM actin, the optimum activation was observed at 0.5 μM VCA or N-WASP. The activation decreased at higher concentrations of VCA or N-WASP (Fig. 4 c). The maximum extent of activation was fourfold higher with VCA than with N-WASP. The effect of N-WASP, but not of VCA, was further stimulated (about threefold) by Cdc42-GTPγS, not by Cdc42-GDP (Fig. 4 d), in agreement with Rohatgi et al. (1999).

In conclusion, in the whole N-WASP protein, the VCA domain is accessible to Arp2/3 complex and capable of activating Arp2/3 function in actin assembly.

IcsA Mimics Cdc42-induced Activation of N-WASP

The recombinant IcsA protein greatly stimulated the N-WASP–Arp2/3-induced polymerization of actin in a concentration-dependent, saturable fashion (Fig. 4 e). In the presence of 20 nM Arp2/3 complex and 130 nM N-WASP, 80% of the maximal polymerization rate was reached upon addition of 30 nM IcsA, indicating that maximal activity is associated with the formation of a ternary Arp2/3–

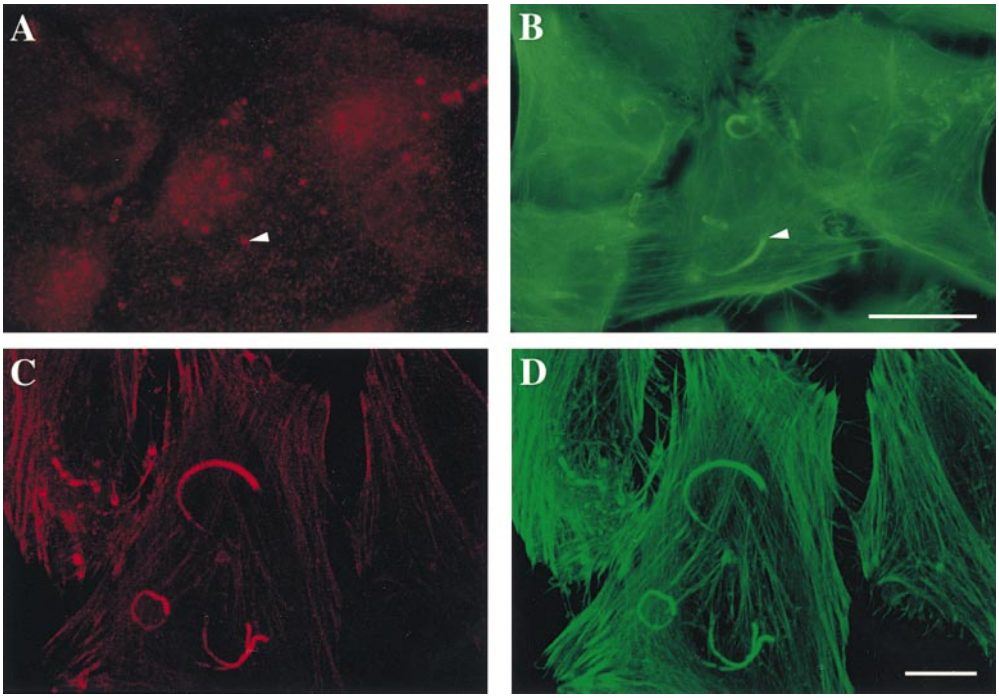

Figure 3. Immunolocalization of N-WASP and Arp2/3 complex in HeLa cells infected with *Shigella* forming actin tails. *Shigella*-infected cells were fixed and immunolabeled with NW011 anti-N-WASP polyclonal antibodies (A) or with AR3 anti-Arp3 polyclonal antibodies (C) and with FITC-phalloidin (B and D). A and B represent the sum of all optical sections and C and D represent a single optical section close to focal plaques. Texas red-coupled secondary antibody was used to detect both immunocomplexes. Localization of N-WASP on the bacterium surface is indicated by an arrowhead. Bars, 10 μm.

N-WASP–IcsA complex in which the equilibrium K_d of IcsA is in the nanomolar range. The activation reached with IcsA was greater than with Cdc42. Interestingly, IcsA by itself did not affect the polymerization of actin alone, but at concentrations as low as 0.1 μM, it activated the Arp2/3 complex to some extent in the absence of N-WASP (control curves in Fig. 4 e), which indicates that IcsA interacts with Arp2/3 complex. In the presence of N-WASP, IcsA, and Arp2/3, a true triangular complex is formed between the three proteins at the surface of *Shigella*, enhancing the stability of the edifice.

The Isolated VCA of N-WASP Binds G-actin and Affects Actin Assembly in a Profilin-like Fashion

The VCA of N-WASP was described as a filament depolymerizing filament severing protein (Miki et al., 1996, 1998b; Suzuki et al., 1998). These conclusions do not appear confirmed in the present work. The interaction of isolated VCA with actin was examined in steady state and kinetic experiments, on the dynamics of pointed and barbed ends separately.

When filament barbed ends are capped by gelsolin, VCA induced a shift in the critical concentration plots (Fig. 5 a). Addition of increasing amounts of VCA to F-actin at a given concentration caused a linear decrease in F-actin at steady state, leading to eventual complete depolymerization at high concentration of VCA. The slope of the plot (Fig. 5 b) was independent of the actin concentration. Hence, VCA behaves like a G-actin sequestering protein when barbed ends are capped. A value of 0.8 ± 0.1 μM was derived for the equilibrium K_d of the VCA–G-actin complex, from analysis of the data in Fig. 5, a and b.

When barbed ends were free, the behavior of VCA was different. No efficient sequestration of actin was observed. In the presence of 5 μM VCA, a modest shift of the critical concentration plots from 0.12 to 0.21 μM unassembled actin was observed, while a 3.5-fold larger shift (up to 0.7 μM unassembled actin) was expected, using the K_d value of 0.8 μM. These results are reminiscent of the effect of profilin in actin assembly (Pantaloni and Carlier, 1993) and they demonstrate that when barbed ends are free, the concentration of ATP–G-actin at steady state is lowered by VCA, suggesting that VCA–actin complex, like profilin–actin, participates in barbed end assembly. Specifically, in the experiment shown in Fig. 5 c, the amount of unassembled actin, $[A]_0$, at steady state is 0.21 μM, which distributes into free G-actin, [A], and VCA–actin complex, [VA]. The concentrations of free G-actin and VCA-actin are linked by the law of mass action: $([A] \cdot ([V]_{total} - [VA]) / [VA] = K_d)$; and by the sum: $[A]_0 = [A] + [VA]$; resulting in a quadratic equation that has a single solution: [A] = 0.03 μM, [VA] = 0.18 μM. The concentration of free actin, thus, appears fourfold lower than 0.12 μM, the value that is measured in the absence of VCA.

Evidence for the participation of VCA–actin complex in barbed end assembly was directly provided by measurements of the rate of filament growth. The rate of elongation from G-actin at pointed ends, initiated by gelsolin–actin complex, was totally inhibited by VCA (Fig. 5 c), confirming that the VCA–actin complex does not polymerize onto pointed ends. In contrast, growth of barbed ends initiated by spectrin–actin seeds, was inhibited only by 30% at saturation by VCA, indicating that the VCA–actin complex associates to barbed ends with a rate constant 30% lower than G-actin (Fig. 5 d). Again, this result is strikingly similar to the one obtained with profilin (Gutsche-Perelroizen et al., 1999). Like profilin, VCA delivers G-actin subunits to growing barbed ends and dissociates from the barbed end after incorporation of actin, in

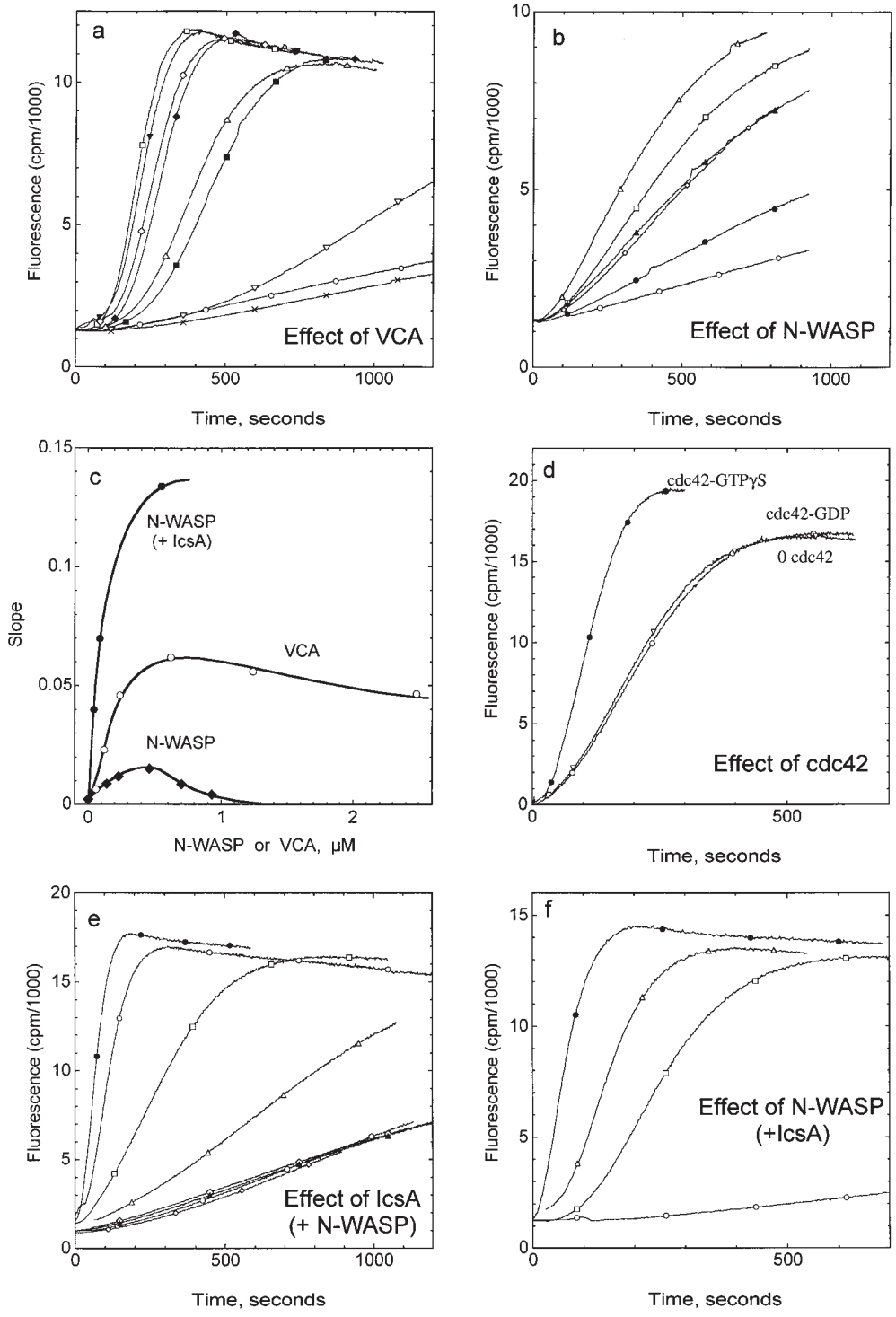

Figure 4. IcsA mimics Cdc42 in activating N-WASP and stimulating actin polymerization by Arp2/3 complex. Mg-G-actin (2.5 μM, 9% pyrenyl-labeled) was induced to polymerize by addition of 0.1 M KCl and 1 mM $MgCl_2$ in the presence or absence of Arp2/3 complex (9.5 nM) and other reagents as indicated. a, VCA activates Arp2/3 complex. ×, Control (actin alone). For all other curves, Arp2/3 (9.5 nM) and VCA are at the following concentrations: ○, 0; ▽, 0.06 μM; △, 0.12 μM; ◇, 0.24 μM; □, 0.62 μM; ▼, 1.24 μM; ◆, 2.48 μM; ■, 3.7 μM. b, N-WASP activates Arp2/3 complex. Same conditions as in a, except N-WASP varied as follows: ○, 0; ◇, 0.115 μM; □, 0.23 μM; △, 0.46 μM; ▲, 0.70 μM; ●, 0.93 μM. c, Dependence of the activation of Arp2/3 on VCA and N-WASP concentrations. The maximum rate of polymerization recorded in panels a, b, and f (in the presence of IcsA) is plotted versus the concentrations of VCA (○) or N-WASP (●). d, Cdc42 activates N-WASP–Arp2/3 complex. Same as in b, with 0.2 μM N-WASP, in the absence (△) or in the presence of GDP-Cdc42 (○) or GTPγS-Cdc42 (●). e, IcsA activates N-WASP–Arp2/3 complex. Actin was polymerized alone (▲); in the presence of 19 nM Arp2/3 (○), 0.25 μM IcsA (◇) or 0.13 μM N-WASP (small ◇); in the presence of Arp2/3 and 0.25 μM IcsA (△); Arp2/3 and 0.13 μM N-WASP (□); Arp2/3, 0.13 μM N-WASP and 30 nM (○), or 0.25 μM (●) IcsA. f, Activation of Arp2/3 complex by N-WASP is more pronounced in the presence of IcsA. Actin was polymerized in the presence of Arp2/3, 0.1 μM IcsA and 0 (○), 0.042 μM (□), 0.087 μM (△), and 0.55 μM (●) N-WASP.

a manner coupled to ATP hydrolysis. The coupling to ATP hydrolysis was demonstrated to be thermodynamically required to account for the decrease in partial critical concentration of actin (Pantaloni and Carlier, 1993).

Spontaneous polymerization of actin was inhibited by VCA, exactly as observed with profilin (data not shown). Hence, VCA–actin complex, like profilin–actin complex, is able to productively associate to barbed ends, but not to nucleate F-actin. This result accounts for the decrease observed in the activation of Arp2/3 complex at high VCA or

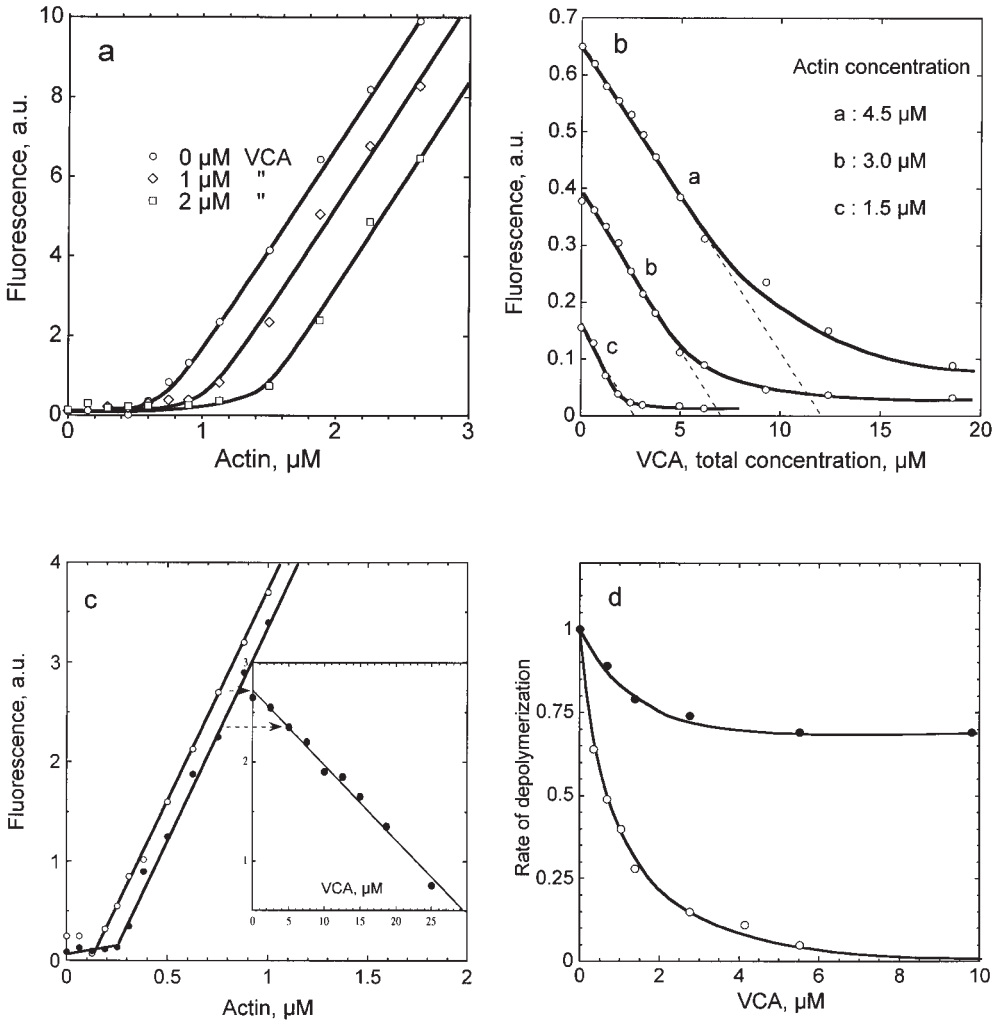

Figure 5. Isolated VCA acts in a profilin-like fashion in actin assembly. a, Critical concentration plots for assembly of gelsolin-capped filaments (gelsolin:actin = 1:300) in the absence (○) or in the presence of VCA at 1 μM (◇) or 2 μM (□). Pyrenyl fluorescence was measured at steady state. b, VCA sequesters actin when barbed ends are capped. Gelsolin-capped F-actin (gelsolin:actin = 1:300, 9% pyrenyl-labeled actin) was incubated overnight at 4.5 μM (a), 3.0 μM (b), and 1.5 μM (c), in the presence of VCA at the indicated concentrations. Pyrenyl fluorescence was measured at steady state. c, VCA does not efficiently sequester actin when barbed ends are free. Critical concentration plots were monitored in the absence (○) and in the presence of 5 μM VCA (●). Inset, Increasing amounts of VCA were added to 0.75 μM F-actin. Pyrenyl fluorescence was monitored at steady state. Note that 30 μM VCA appear required to depolymerize 0.6 μM F-actin when barbed ends are capped, whereas 4.6 μM VCA would be expected to be required, assuming a pure sequestering activity and a K_d of 0.8 μM for the VCA–G-actin complex. d, VCA–G-actin does not assemble onto pointed ends, but participates in barbed end assembly with the same kinetic parameters as profilin–actin. Rates of pointed end assembly from gelsolin–actin (○) and of barbed end assembly from spectrin–actin seeds (●) were measured at 1 μM G-actin and the indicated concentrations of VCA.

N-WASP concentration (Fig. 4, a and b), which correlates with the saturation of G-actin by VCA. At low concentrations, VCA-actin interacts with Arp2/3 complex to enhance nucleation, but when all G-actin is bound to VCA, actual inhibition of nucleation occurs.

The NH_2-terminal Domain of N-WASP Binds and Stabilizes F-Actin in an IcsA-enhanced Fashion

Full-length N-WASP did not display the G-actin sequestering activity of VCA, when barbed ends were capped by gelsolin. No depolymerization of gelsolin-capped F-actin was measured at steady state, and only weak inhibition in the rate of growth at the pointed ends of gelsolin-capped filaments was detected by addition of N-WASP. Instead, N-WASP bound to F-actin and stabilized the filaments, as shown by the observed decrease in critical concentration (Fig. 6 a). A slight decrease in the slope of the pyrenyl fluorescence critical concentration plots indicated that the fluorescence of F-actin was partially quenched upon binding N-WASP. The binding to F-actin and the decrease in critical concentration were also observed in a sedimentation assay (Fig. 6 a, inset). The NH_2-terminal fragment of N-WASP protein (Nt, residues 1–276) stabilized the filaments and affected the slope of the critical concentration plots of gelsolin-capped filaments exactly like the full-length protein (Fig. 6 a), and bound to F-actin in sedimentation assays, which indicates that the Nt contains the F-actin binding site. The affinity of N-WASP for F-actin was roughly estimated to 2 to 5 10^5 M^{-1} from these data. The binding to F-actin presumably counteracted and prevented observation of the sequestering activity of the COOH-terminal part of N-WASP in solutions of F-actin.

When barbed ends are free, the critical concentration is low (0.1 μM), hence, the stabilizing effect of N-WASP (decrease in critical concentration) was best observed in the presence of a sequestering protein like thymosin β4. The amount of unassembled actin at steady state then is ampli-

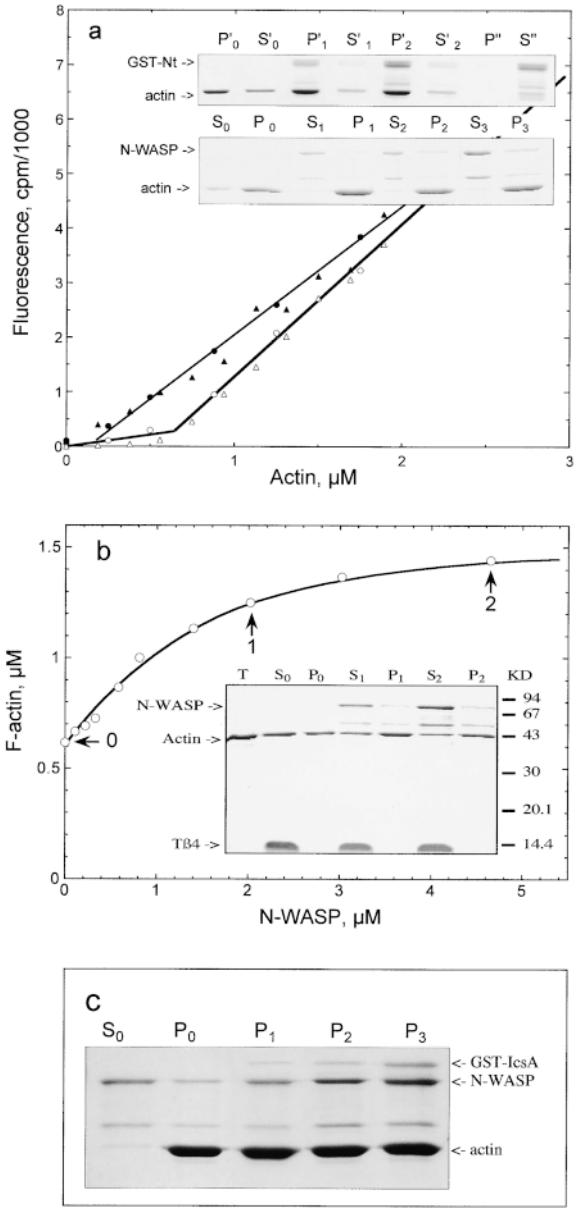

Figure 6. An NH_2-terminal region in N-WASP binds F-actin in an IcsA-enhanced fashion. a, Critical concentration plots for assembly of gelsolin-capped filaments in the absence (○ and △) and in the presence (●) of 3.6 μM N-WASP, or 2 μM GST–N-WASP–Nt fragment (▲). Inset, SDS-PAGE patterns of the pellets (P) and supernatants (S) of samples of 2 μM gelsolin-capped F-actin incubated in the presence of 0 (P_0 and S_0), 1.6 μM (P_1 and S_1), 2.12 μM (P_2 and S_2), and 3.6 μM (P_3 and S_3) N-WASP, and 0 (P'_0 and S'_0), 1 μM (P'_1 and S'_1), 2 μM (P'_2 and S'_2) GST–N-WASP–Nt fragment. P′′ and S′′ represent the pellet and supernatant of 2 μM GST–N-WASP–Nt alone. Note the decrease in actin in the supernatants, and the associated binding of N-WASP and its NH_2-terminal fragment to F-actin. b, N-WASP promotes actin polymerization from a pool of Tβ4–actin complex when barbed ends are free. N-WASP was incubated at the indicated concentrations with 2 μM F-actin (9% pyrenyl-labeled) in the presence of 30 μM Tβ4. Pyrenyl fluorescence was measured at steady state, and converted in F-actin concentrations using a critical concentration plot carried out in parallel using the same F-actin solution. Inset, SDS-PAGE pattern of the pellets (P) and supernatants (S) of sedimented samples (marked with an arrow in the main frame) containing 2 μM F-actin, 30 μM Tβ4, and 0 (P_0 and S_0), 2.09 μM (P_1 and S_1), and 4.65 μM (P_2 and S_2) N-WASP, respectively. c, IcsA strengthens the binding of N-WASP to F-actin. SDS-PAGE patterns of the pellets (P) and supernatants (S) of samples of F-actin (2 μM) incubated in the presence of 2 μM N-WASP and in the absence (P_0 and S_0) or in the presence of 0.15 μM (P_1), 0.3 μM (P_2), and 0.6 μM (P_3) GST–IcsA.

fied by the sequestering effect of thymosin β4, making any change in critical concentration easily measurable. The sequestering effect of thymosin β4 was drastically reduced by N-WASP, as the result of the decrease in critical concentration (Fig. 6 b). Addition of 30 μM thymosin β4 to 2 μM F-actin caused depolymerization of 1.28 μM actin into thymosin β4–actin complex, consistent with a value of $0.1 \cdot (30 - 1.28) / 1.28 = 2.2$ μM for the K_d of the thymosin β4–actin complex. Upon addition of N-WASP to this solution, the concentration of F-actin at steady state increased. At saturation by N-WASP, only 0.5 μM actin was unassembled, which, by solving the quadratic equation expressing the combination of the laws of mass conservation and mass action, corresponded to 0.47 μM thymosin β4–actin complex and 0.03 μM G-actin. Hence, the barbed end critical concentration was decreased three- to fourfold by N-WASP. Sedimentation assays confirmed the conclusions derived from fluorescence measurements (Fig. 6 b, inset). In the presence of IcsA, the binding of N-WASP to F-actin was strengthened (Fig. 6 c), and N-WASP–bound IcsA then cosedimented with F-actin. In conclusion, binding of IcsA to N-WASP enhances the affinity of both its COOH-terminal domain for Arp2/3 complex and its NH_2-terminal domain for F-actin.

Removal of VASP Does Not Affect Actin-based Movement of Shigella

To test the postulate that the binding of vinculin to IcsA would serve to recruit VASP (Laine et al., 1997), which would have the same function in *Shigella* and *Listeria* movement, immunodepletion of VASP in platelet extracts was performed as described (Laurent et al., 1999). Total depletion of VASP was checked by immunoblotting. The movement of *E. coli* (IcsA) precoated with N-WASP was not affected by removal of VASP (Table I). Control samples were prepared in parallel to verify that *Listeria*, in contrast, did not move at all in VASP-depleted extracts, in agreement with previous observations (Laurent et al., 1999). In conclusion, the putative vinculin–VASP interaction is unlikely to play a role in *Shigella* movement.

Profilin Is Not Required, but Enhances Actin-based Movement of Shigella Via Binding to Actin, Not to Proline-rich Proteins

Depletion of profilin from platelet extracts by extensive poly-L-proline chromatography led to a 40% decrease in the rate of propulsion of both *Listeria* and *E. coli* (IcsA). Add-back of pure bovine spleen profilin (1 μM) restored 80% of the rate measured in mock-depleted extracts. It has been postulated (Suetsugu et al., 1998; Suzuki et al., 1998) that binding of profilin to the proline-rich regions of N-WASP could play a functional role in filopodium extension, which is, like *Shigella* movement, mediated by

Table I. Role of Profilin and VASP in the Movement of E. coli (IcsA)

Experiment	Conditions	Rate of movement
		μm/min
A	Full platelet extract	3.1 ± 0.2
VASP depletion	Mock-depleted extract	2.6 ± 0.6
	VASP-depleted extract	2.6 ± 0.8
	VASP-depleted extract + 1 μM purified recombinant VASP	2.3 ± 0.1
B	Full platelet extract	2.5 ± 0.2
Profilin depletion	Mock-depleted extract	2.0 ± 0.3
	Profilin-depleted extract	1.3 ± 0.1
	Profilin-depleted extract + 1 μM wild-type profilin	1.7 ± 0.1
	Profilin-depleted extract + 1 μM H133S-mutant profilin	1.7 ± 0.2

A, VASP is not involved in movement of *E. coli* (IcsA). Platelet extracts were depleted from VASP as described in Materials and Methods, and assayed for movement of N-WASP-coated *E. coli* (IcsA). B, Profilin accelerates the movement of *E. coli* (IcsA) in a fashion that does not require its binding to proline-rich proteins. Profilin was depleted from 50 μl of platelet extracts as described in Materials and Methods. The extracts were assayed for motility of N-WASP–coated *E. coli* (IcsA). Rates of movement were measured using a Hamamatsu image analyzer. Average rates were derived from the distances moved over a period of 1 min (10 ± 2 rate measurements). Error represents calculated SD.

N-WASP-induced actin polymerization. To test this possibility, the add-back of profilin was performed using H133S-mutated profilin that fails to bind to poly-L-proline (Bjorkegren-Sjogren et al., 1997). We first checked that the mutated profilin bound actin in a functional fashion strictly identical to either the bovine profilin or the recombinant human wild-type profilin. In brief, H133S profilin sequestered actin when barbed ends were capped, participated in barbed end assembly when they were uncapped, and the H133S profilin–actin complex associated to barbed ends in a growth assay (Gutsche-Perelroizen et al., 1999) at the same rate as the wild-type profilin–actin complex (data not shown). H133S profilin enhanced the rate of bacteria movement in profilin-depleted extracts to the exact same extent as bovine profilin in three reproducible experiments (Table I), demonstrating that, by interacting directly with actin and not with a proline-rich protein, profilin enhances actin-based motility. Accordingly, we recently showed (Laurent et al., 1999) that the function of profilin in *Listeria* movement is independent of VASP, another proline-rich protein also initially thought to act by recruiting profilin.

Discussion

The stimulation of local actin assembly by Arp2/3 complex in response to different stimuli is thought to be pivotal in the generation of a large diversity of cellular extensions (lamellipodia, filopodia, neural growth cone, etc.), suggesting that a variety of connectors must link the different members of the Rho family to the Arp2/3 complex and activate actin polymerization by a common mechanism, with different partners. Our work shows that lessons can be learned from *Shigella* to understand the molecular mechanism of Cdc42-induced filopodium extension mediated by actin polymerization.

The IcsA–N-WASP–Arp2/3 Ternary Complex Is Responsible for the Stimulation of Actin Assembly at the Surface of Shigella

Recently, Rohatgi et al. (1999) showed that N-WASP relays Cdc42 signals and directly activates the Arp2/3 complex in *Xenopus* egg extracts and in vitro with purified N-WASP and Arp2/3 complex. We extend this work to show that the *Shigella* IcsA protein mimics Cdc42, to greatly enhance the affinity of N-WASP for Arp2/3 complex, thus assembling a tight IcsA–N-WASP–Arp2/3 ternary complex at the bacterial surface, in a conformation that has maximal activity in actin assembly. N-WASP activation by IcsA explains why *Shigella* actin-based motility is independent of the Rho GTPases (Mounier et al., 1999).

Our findings, combined with results from other laboratories (Machesky and Insall, 1998; Miki et al., 1998b; Rohatgi et al., 1999), can be summarized using a thermodynamic scheme expressing that: both Arp2/3 complex and N-WASP exist in solution in two conformations, inactive (X) and active (X*; Scheme 1). The active form of Arp2/3 complex (A*) stimulates actin polymerization. The active form of N-WASP (W*) exposes two functionally active domains involved in actin-based motility, which may be masked in the inactive state by intramolecular interaction (Miki and Takenawa, 1998; Miki et al., 1998b). The VCA binds Arp2/3 complex and G-actin, and the NH_2-terminal domain binds F-actin. Our data (Fig. 6 b) indicate that the F-actin binding site is most likely located in the WH1 domain, which also interacts with the verprolin homologue WIP. This formulation accounts for the fact that the Arp2/3 complex by itself has a weak nucleating activity (Mullins et al., 1998; Machesky et al., 1999) and that N-WASP by itself is able to bind F-actin and G-actin

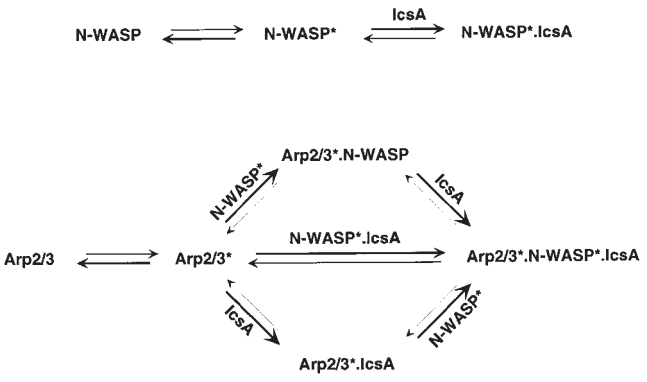

Scheme 1

weakly (this work). Binding of IcsA (I) to N-WASP shifts the N-WASP equilibrium toward the W* form, exposing the VCA domain and the F-actin binding domain, thus enhancing the affinity of N-WASP for active Arp2/3 complex (Fig. 4 e) and F-actin (Fig. 6 c).

Binding of N-WASP to Arp2/3 complex shifts the Arp2/3 equilibrium toward the A* form, increasing the amount of nucleating complex. It is implicit here that to nucleate actin polymerization, Arp2/3 complex binds G-actin.

In the presence of IcsA and N-WASP, the Arp2/3 complex equilibrium is maximally shifted toward the A* form, in a triangular A*–W*–I complex. In this complex, protein–protein bonds are formed between the three partners (A-W, W-I, and A-I). Hence, each of the three components increases the stability of the complex.

It is very likely that in vivo the actin-polymerization machinery is highly integrated and works on an all-or-none basis, i.e., the Arp2/3 complex switches from an inactive to a fully active form upon interacting with the COOH-terminal region of N-WASP, which itself is exposed only when Cdc42 has switched to its active conformation by binding GTP. Separating the components of this machinery by purification may cause structural alterations that partially unmask the protein interfaces normally buried in the inactive state. Detailed studies of the effect of solution variables on the activity of pure Arp2/3 complex will certainly help to understand the physical–chemical basis of N-WASP and Arp2/3 activation.

VCA has a high affinity for Arp2/3 complex (a rough estimate of 10^7 M^{-1} can be derived from the polymerization curves), allowing easy depletion of Arp2/3 from extracts and a straightforward purification procedure by affinity chromatography. At variance with a previous report (Suzuki et al., 1998), VCA does not appear to bind to IcsA and elicit actin polymerization at the surface of *Shigella*. The reason for the discrepancy with Suzuki et al. (1998) remains obscure, but may relate to the different methods used to probe the interaction. We conclude that VCA is not sufficient for IcsA binding and that this interaction probably also requires residues present outside of the VCA domain.

Since WASP and N-WASP are very similar in sequence, it is surprising that WASP, which is abundant in platelets, does not appear able to bind IcsA. A possible explanation is that WASP in platelets may be in strong interaction with other ligands, competing with IcsA binding. It may be noted, in this respect, that while the CRIB domains of WASP and N-WASP are very similar in sequence, differences exist in the binding of Cdc42-Y40C (Miki et al., 1998b).

Whether Cdc42 and IcsA directly compete for the same site to activate N-WASP is not known, but raises an interesting issue concerning the possible multiple ways of activation of N-WASP. The interface of the CRIB domain of N-WASP with GMPPCP-Cdc42 is known from NMR studies (Abdul-Manan et al., 1999). It is also known that the glycine-rich regions of IcsA are involved in the association with N-WASP (Suzuki et al., 1998). The structural aspects of N-WASP activation await more detailed investigation. Like *Shigella*, other pathogen model systems may help discover the multiple effectors linking Arp2/3 complex to different signaling pathways.

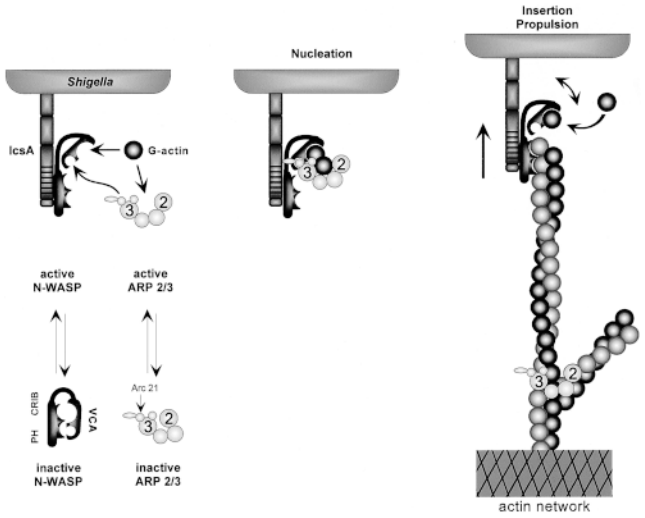

Figure 7. Working model for actin-based movement of *Shigella*. Left, Binding of N-WASP to IcsA at *Shigella* surface activates the connector, exposing the Arp2/3 complex, G-actin, and F-actin binding sites. Center, Nucleation: interaction of VCA with G-actin and Arp2/3 complex in a ternary complex in which the G-actin is positioned at the barbed end. Right, Barbed end growth and movement: the VCA domain of N-WASP shuttles G-actin subunits to the growing barbed end. The filament is maintained in close vicinity to the bacterium surface by binding to the NH_2-terminal domain of N-WASP.

The Arp2/3–N-WASP Complex Works with Actin as a Motor at the Surface of Shigella

Analysis of the interaction of the COOH-terminal and NH_2-terminal domains of N-WASP with actin provides insight in the mechanism by which actin polymerizes at the surface of *Shigella*. The two domains of N-WASP that become exposed upon binding to IcsA fulfill different functions. The COOH-terminal domain binds G-actin and Arp2/3 complex. The nucleation and filament branching activities of Arp2/3 imply that G-actin binds to Arp2/3 complex, perhaps by interacting with Arp2 or Arp3 (Pantaloni, D., manuscript in preparation). We propose, in agreement with Machesky and Insall (1998) and Rohatgi et al. (1999), that the binding of G-actin in the nucleation complex is facilitated by association of the VCA domain to Arp2/3 complex, because in the VCA–actin complex, actin is positioned in the right orientation to interact with Arp2/3, in the structure of a barbed end nucleus, hence the free energy of G-actin binding to Arp2/3 is lowered.

Second, in the filament elongation step, while the VCA domain functions like profilin in barbed end assembly, shuttling actin subunits onto growing barbed ends, the NH_2-terminal domain of N-WASP maintains the filament in the vicinity of *Shigella* surface. We propose that the two domains of N-WASP work together with actin as expected for a motor of insertional polymerization at the surface of *Shigella* (Fig. 7). Note that it is the treadmilling of actin filaments (which is a dissipative process) that supports unidirectional filament growth and promotes steady movement. N-WASP acts as a molecular ratchet that transduces actin polymerization into force. N-WASP is the first protein described thus far that possesses an integrated profilin-like

function and locally lowers the critical concentration of G-actin. Whether other proteins share the same property in different cellular contexts is an exciting possibility.

The observed localization of Arp2/3 complex in the actin tail of *Listeria* (Welch et al., 1997) and of *Shigella* (Fig. 3 in the present work) correlates with its localization in the lamellipodium (Bailly et al., 1999; Svitkina and Borisy, 1999). In the present work, the combination of motility assays with the biochemical analysis of the effects of Arp2/3 complex and N-WASP on actin polymerization brings a functional insight into the immunolocalization studies. While N-WASP remains bound to IcsA as the bacterium is moving (Fig. 3), the Arp2/3 complex is activated by interacting with N-WASP transiently to nucleate and branch the filaments, then Arp2/3 complex remains incorporated in the actin meshwork as it is formed. We conclude that the Arp2/3 complex present in the actin tail (and in the lamellipodium) is no longer activated by N-WASP. This view is quite different from the currently expressed one (Mullins et al., 1998; Machesky et al., 1999). The *Shigella* bacterial model, therefore, proves to be a good tool to understand the mechanics of lamellipodium extension.

Comparison of the *Listeria* and *Shigella* actin-based motility mechanisms provides interesting information on the different strategies available to induce actin assembly. *Listeria* does not harness a cellular activator of Arp2/3 complex. Instead, the ActA protein itself elicits the two functions of activated N-WASP. The central proline-rich domain of ActA binds VASP, which in turn binds F-actin, thus mediating the attachment of the filaments to the bacterium, as does the NH_2-terminal domain of N-WASP in *Shigella*. Whether the NH_2-terminal domain of ActA, which activates nucleation by Arp2/3 complex, acts like VCA by interacting with the p21-Arc subunit of Arp2/3 complex and with G-actin, possibly in a profilin-like fashion, is an open issue that may be of general relevance in the stimulation of actin assembly and which deserves investigation. Remarkably, the NH_2-terminal domain of ActA contains the acidic sequence DEWEE homologue of the DEWED in the extreme COOH-terminal region A of VCA, and a sequence KKRRKAIASS similar to the QKRSKAIHSS sequence in the cofilin homology region of VCA, but does not contain the verprolin homology regions present in VCA. The possibility is raised that Arp2/3 complex is activated in a similar way by different effectors.

VASP Is Not Involved in Shigella Movement

Removal of VASP from platelet extracts does not affect the movement of *Shigella*, while VASP is essential in the propulsion of *Listeria*. This result rules out the postulated mechanism according to which VASP would work, in both *Shigella* and *Listeria* systems, as a profilin recruiter, to enhance actin assembly in an actin-based motility (ABM) complex (Zeile et al., 1998). Incidentally, the physical relevance of that mechanism was questionable, since diffusion of profilin-actin is very fast and dissociation of profilin from a proline-rich target would introduce a kinetically limiting step in filament assembly. Overall, our results are in general agreement with the conclusion derived by Goldberg (1997) that vinculin, hence the vinculin–VASP interaction, is not required in *Shigella* motility. Our data further show that the function of profilin in actin-based *Shigella* movement is mediated by binding actin directly, without interacting with the proline-rich region of N-WASP. Similarly, we demonstrated that the function of profilin in *Listeria* movement is independent of VASP (Laurent et al., 1999). VASP in *Listeria* and N-WASP in *Shigella* mediate attachment of the actin tail to the bacterial surface. Hence, the mechanisms of movement of these two pathogens are similar in their physical principles, and some of the operators are the same (Arp2/3 complex and actin), whereas some functions are elicited by different players.

From Actin Polymerization to Movement

Although the interaction of IcsA with N-WASP is essential in generating *Shigella* motility, N-WASP-coated bacteria fail to actively move in a solution of F-actin at steady state in the presence of Arp2/3 complex. As pointed out earlier (Carlier, 1998), regulatory factors that maintain G-actin at a high steady state concentration, by regulating the dynamics of actin assembly, are important missing ingredients in the reconstitution of movement (Loisel et al., 1999).

We thank Dr. Sally Zigmond for a generous gift of recombinant wild-type and H133S profilins, and Dr. Jürgen Wehland for anti-VASP and anti-Arp3 antibodies.

M.-F. Carlier acknowledges partial support from the Association pour la Recherche contre le Cancer (ARC), the Association Française contre les Myopathies (AFM), and a Human Frontier in Science grant. P.J. Sansonetti acknowledges support from Ministère de la Recherche, Direction des Recherches et Techniques (DRET), and a grant from the Fondation Louis Jeantet de Médecine. The confocal microscope was bought with a donation from Marcel and Liliane Pollack. C. Egile is supported by the Fondation pour la Recherche Médicale. T.P. Loisel is supported by a fellowship from the Natural Sciences and Engineering Research Council of Canada.

Submitted: 19 May 1999
Revised: 22 July 1999
Accepted: 20 August 1999

References

Abdul-Manan, N., B. Aghazadeh, G.A. Liu, A. Majumdar, O. Ouerfelli, K.A. Siminovitch, and M.K. Rosen. 1999. Structure of Cdc42 in complex with the GTPase-binding domain of the Wiskott-Aldrich syndrome protein. *Nature.* 399:379–383.

Bailly, M., F. Macaluso, M. Cammer, A. Chan, J.E. Segall, and J.S. Condeelis. 1999. Relationship between Arp2/3 complex and the barbed ends of actin filaments at the leading edge of carcinoma cells after EGF stimulation. *J. Cell Biol.* 145:331–346.

Bear, J.E., J.F. Rawls, and C.L. Saxe III. 1998. SCAR, a WASP-related protein, isolated as a suppressor of receptor defects in late *Dictyostelium* development. *J. Cell Biol.* 142:1325–1335.

Beckerle, M.C. 1998. Spatial control of actin filament assembly: lessons from *Listeria*. *Cell.* 95:741–748.

Bernardini, M.L., J. Mounier, H. d'Hauteville, M. Coquis-Rondon, and P. Sansonetti. 1989. Identification of IcsA, a plasmid locus of *Shigella flexneri* that governs bacterial intra and intercellular spread through interaction with F-actin. *Proc. Natl. Acad. Sci. USA*. 86:3867–3871.

Bi, E., and S.H. Zigmond. 1999. Actin polymerization: where the WASP stings. *Curr. Biol.* 9:R160–R163.

Bjorkegren-Sjogren, C., E. Korenbaum, P. Nordberg, U. Lindberg, and R. Karlsson. 1997. Isolation and characterization of two mutants of human profilin I that do not bind poly(L-proline). *FEBS Lett.* 418:258–264.

Carlier, M.-F. 1998. Control of actin dynamics. *Curr. Opin. Cell Biol.* 10:45–51.

Carlier, M.-F., V. Laurent, J. Santolini, D. Didry, R. Melki, Y. Hong, G.-X. Xia, N.-H. Chua, and D. Pantaloni. 1997. ADF/cofilin enhances the turnover of actin filaments. Implication in actin-based motility. *J. Cell Biol.* 136:1307–1322.

Casella, J.F., D.J. Maack, and S. Lin. 1986. Purification and initial characteriza-

tion of a protein from skeletal muscle that caps the barbed ends of actin filaments. *J. Biol. Chem*. 261:10915–10921.

Derry, J.M., H.D. Ochs, and U. Francke. 1994. Isolation of a novel gene mutated in Wiskott-Aldrich syndrome. *Cell*. 78:635–644.

Domann, E., J. Wehland, M. Rhode, S. Pistor, M. Hartl, W. Goebel, M. Leismeister-Wächter, M. Wuenscher, and T. Chakraborty. 1992. A novel bacterial virulence gene in *Listeria monocytogenes* required for host cell microfilament interaction with homology to the proline-rich region of vinculin. *EMBO (Eur. Mol. Biol. Organ.) J.* 11:1981–1990.

Goldberg, M.B. 1997. *Shigella* actin-based motility in the absence of vinculin. *Cell Motil. Cytoskeleton*. 37:44–53.

Goldberg, M.B., and J.A. Theriot. 1995. *Shigella flexneri* surface protein IcsA is sufficient to direct actin-based motility. *Proc. Natl. Acad. Sci. USA*. 92:6572–6576.

Goldberg, M.B., O. Barzu, C. Parsot, and P. Sansonetti. 1993. Unipolar localization and ATPase activity of IcsA, a *Shigella flexneri* protein involved in intracellular movement. *J. Bacteriol*. 175:2189–2196.

Gutsche-Perelroizen, I., J. Lepault, A. Ott, and M.-F. Carlier. 1999. Filament assembly from profilin-actin. *J. Biol. Chem*. 274:6234–6243.

Higley, S., and M. Way. 1997. Actin and cell pathogenesis. *Curr. Opin. Cell Biol*. 9:62–69.

Kocks, C., E. Gouin, M. Tabouret, P. Berche, H. Ohayon, and P. Cossart. 1992. *L. monocytogenes*-induced assembly requires actA gene product, a surface protein. *Cell*. 68:521–531.

Kocks, C., J.-B. Marchand, E. Gouin, H. d'Hauteville, P. Sansonetti, M.-F. Carlier, and P. Cossart. 1995. The unrelated surface proteins ActA of *Listeria monocytogenes* and IcsA of *Shigella flexneri* are sufficient to confer actin-based motility on *Listeria innocua* and *E. coli* respectively. *Mol. Microbiol*. 18:413–423.

Kozma, R., S. Ahmed, A. Best, and L. Lim. 1995. The ras-related protein Cdc42Hs and bradykinin promote formation of peripheral actin microspikes and filopodia in Swiss 3T3 fibroblasts. *Mol. Cell. Biol*. 15:1942–1952.

Laine, R.O., W. Zeile, F. Kang, D.L. Purich, and F.S. Southwick. 1997. Vinculin proteolysis unmasks an ActA homolog for actin-based *Shigella* motility. *J. Cell Biol*. 138:1255–1264.

Laurent, V., and M.-F. Carlier. 1997. Use of platelet extracts for actin-based motility of *Listeria monocytogenes*. *In* Cell Biology Laboratory Handbook. E. Celis, editor. Academic Press, San Diego, CA. 359–365.

Laurent, V., T.P. Loisel, B. Harbeck, A. Wehman, L. Gröbe, B.M. Jockusch, J. Wehland, F.B. Gertler, and M.-F. Carlier. 1999. Role of the proteins of the Ena/VASP family in actin-based motility of *Listeria monocytogenes*. *J. Cell Biol*. 144:1245–1258.

Lechler, T., and R. Li. 1997. In vitro reconstitution of cortical actin assembly sites in budding yeast. *J. Cell Biol*. 138:95–103.

Lett, M.C., C. Sasakawa, N. Okada, T. Sakai, S. Makino, M. Yamada, K. Komatsu, and M. Yoshikawa. 1989. VirG, a plasmid-coded virulence gene of *Shigella flexneri*: identification of the virG protein and determination of the complete coding sequence. *J. Bacteriol*. 171:353–359.

Li, R. 1997. Bee1, a yeast protein with homology to Wiskott-Aldrich syndrome protein, is critical for the assembly of cortical actin cytoskeleton. *J. Cell Biol*. 136:649–658.

Loisel, T.P., R. Boujemaa, D. Pantaloni, and M.-F. Carlier. 1999. Reconstitution of actin-based motility of *Listeria* and *Shigella* from pure proteins. *Nature*. In press.

Ma, L., C. Cantley, P.A. Janmey, and M.W. Kirschner. 1998a. Corequirement of specific phosphoinositides and small GTP-binding protein Cdc42 in inducing actin assembly in *Xenopus* egg extracts. *J. Cell Biol*. 140:1125–1136.

Ma, L., R. Rohatgi, and M.W. Kirschner. 1998b. The Arp2/3 complex mediates actin polymerization induced by the small GTP-binding protein Cdc42. *Proc. Natl. Acad. Sci. USA*. 95:15362–15367.

Machesky, L.M., and R.H. Insall. 1998. Scar1 and the related Wiskott-Aldrich syndrome protein, WASP, regulate the actin cytoskeleton through the Arp2/3 complex. *Curr. Biol*. 8:1347–1356.

Machesky, L.M., R.D. Mullins, H.N. Higgs, D.A. Kaiser, L. Blanchoin, R.C. May, M.E. Hall, and T.D. Pollard. 1999. Scar, a WASp-related protein, activates dendritic nucleation of actin filaments by the Arp2/3 complex. *Proc. Natl. Acad. Sci. USA*. 96:3739–3744.

Marchand, J.-B., P. Moreau, A. Paoletti, P. Cossart, M.-F. Carlier, and D. Pantaloni. 1995. Actin-based movement of *Listeria monocytogenes* in *Xenopus* egg extracts is due to the maintenance of uncapped barbed ends at the bacterium surface. *J. Cell Biol*. 130:331–343.

Miki, H., and T. Takenawa. 1998. Direct binding of the verprolin-hology domain in N-WASP to actin is essential for cytoskeletal reorganization. *Biochem. Biophys. Res. Commun*. 243:73–78.

Miki, H., K. Miura, and T. Takenawa. 1996. N-WASP, a novel actin-depolymerizing protein, regulates the cortical cytoskeletal rearrangement in a PIP_2-dependent manner downstream of tyrosine kinases. *EMBO (Eur. Mol. Biol. Organ.) J*. 15:5326–5335.

Miki, H., S. Suetsugu, and T. Takenawa. 1998a. WAVE, a novel WASP-family protein involved in actin reorganization induced by rac. *EMBO (Eur. Mol. Biol. Organ.) J*. 17:6932–6941.

Miki, H., T. Sasaki, Y. Takai, and T. Takenawa. 1998b. Induction of filopodium formation by a N-WASP-related actin-depolymerizing factor. *Nature*. 391: 93–96.

Mounier, J., V. Laurent, A. Hall, P. Fort, M.-F. Carlier, P.J. Sansonetti, and C. Egile. 1999. Rho family GTPases control entry of *Shigella flexneri* into epithelial cells but not intracellular motility. *J. Cell Sci*. 112:2069–2080.

Mullins, R.D., J.A. Heuser, and T.D. Pollard. 1998. The interaction of Arp2/3 complex with actin: nucleation, high affinity pointed end capping and formation of branching networks of actin filaments. *Proc. Natl. Acad. Sci. USA*. 95: 6181–6186.

Nhieu, G.T., and P.J. Sansonetti. 1999. Mechanism of *Shigella* entry into epithelial cells. *Curr. Opin. Microbiol*. 2:51–55.

Niebuhr, K., F. Ebel, R. Frank, M. Reinhardt, E. Domann, U.D. Carl, U. Walter, F.B. Gertler, J. Wehland, and T. Chakraborty. 1997. A novel proline-rich motif present in ActA and cytoskeletal proteins is the ligand for the EVH1 domain, a protein module present in the Ena/VASP family. *EMBO (Eur. Mol. Biol. Organ.) J*. 16:5433–5444.

Nobes, C.D., and A. Hall. 1995. Rho, Rac, and Cdc42 GTPases regulate the assembly of multimolecular focal complexes associated with actin stress fibers, lamellipodia, and filopodia. *Cell*. 81:53–62.

Pantaloni, D., and M.-F. Carlier. 1993. How profilin promotes actin filament assembly in the presence of thymosin β4. *Cell*. 75:1007–1014.

Prevost, M.-C., M. Lesourd, M. Arpin, F. Vernel, J. Mounier, R. Hellio, and P. Sansonetti. 1992. Unipolar reorganization of F-actin layer at bacterial division and bundling of actin filaments by plastin correlate with movement of *Shigella flexneri* within HeLa cells. *Infect. Immun*. 60:4088–4099.

Ramesh, N., I.M. Anton, N. Martinez-Quiles, and R.S. Geha. 1999. Waltzing with WASP. *Trends Cell Biol*. 9:15–19.

Ressad, F., D. Didry, C. Egile, D. Pantaloni, and M.-F. Carlier. 1999. Control of the turnover and length distribution of actin filaments by ADF/cofilin in the presence of capping proteins and Arp2/3 complex. *J. Biol. Chem*. 274:20970–20976.

Rohatgi, R., M. Le, H. Miki, M. Lopez, T. Kichhausen, T. Takenawa, and M.W. Kirschner. 1999. The interaction between N-WASP and the Arp2/3 complex links Cdc42-dependent signals to actin assembly. *Cell*. 97:221–231.

Smith, G.A., J.A. Theriot, and D.A. Portnoy. 1996. The tandem repeat domain in the *Listeria monocytogenes* ActA protein controls the rate of actin-based motility, the percentage of moving bacteria, and the localization of VASP and profilin. *J. Cell Biol*. 135:647–660.

Suetsugu, S., H. Miki, and T. Takenawa. 1998. The essential role of profilin in the assembly of actin for microspike formation. *EMBO (Eur. Mol. Biol. Organ.) J*. 17:6516–6526.

Suzuki, T., S. Saga, and C. Sasakawa. 1996. Functional analysis of *Shigella* VirG domains essential for interaction with vinculin and actin-based motility. *J. Biol. Chem*. 271:21878–21885.

Suzuki, T., H. Miki, T. Takenawa, and C. Sasakawa. 1998. Neural Wiskott-Aldrich syndrome protein is implicated in the actin-based motility of *Shigella flexneri*. *EMBO (Eur. Mol. Biol. Organ.) J*. 17:2767–2776.

Svitkina, T.M., and G.G. Borisy. 1999. Arp2/3 complex and actin depolymerizing factor/cofilin in dendritic organization and treadmilling of actin filament array in lamellipodia. *J. Cell Biol*. 145:1009–1026.

Welch, M.D., A. Iwamatsu, and T.J. Mitchison. 1997. Actin polymerization is induced by the Arp2/3 complex at the surface of *Listeria monocytogenes*. *Nature*. 385:265–269.

Welch, M.D., J. Rosenblatt, J. Skoble, D.A. Portnoy, and T.J. Mitchison. 1998. Interaction of human Arp2/3 complex and the *Listeria monocytogenes* ActA protein in actin filament nucleation. *Science*. 281:105–108.

Winter, D., T. Lechler, and R. Li. 1999. Activation of the Arp2/3 complex by Bee1p, a WASP-family protein. *Curr. Biol*. 9:501–504.

Zeile, W.L., R.C. Condit, J.I. Lewis, D.L. Purich, and F.S. Southwick. 1998. Vaccinia locomotion in host cells: evidence for the universal involvement of actin-based motility sequences ABM-1 and ABM-2. *Proc. Natl. Acad. Sci. USA*. 95:13917–13922.

Zigmond, S.H., M. Joyce, C. Yang, K. Brown, M. Huang, and M. Pring. 1998. Mechanism of Cdc42-induced actin polymerization in neutrophil extracts. *J. Cell Biol*. 142:1001–1012.